C 139

Stars as Suns: Activity, Evolution, and Planets
IAU Symposium, Vol. 219, 2004
A. K. Dupree and A. O. Benz, Eds.

Understanding Solar Variability as Groundwork for Planet Transit Detection

Andrey D. Seleznyov, Natalie A. Krivova, and Sami K. Solanki

Max-Planck-Institut für Aeronomie, Katlenburg-Lindau, Germany

Abstract. Detection of planetary transits holds the greatest promise for the search of extrasolar terrestrial planets. However, intrinsic stellar variability can mask real transits or lead to 'false' planet transit detections. Understanding the origin of stellar variability can help to estimate the minimum sizes of planets detectable with this technique around different types of stars and to identify the best wavelength range for such measurements. The only star for which data with sufficient photometric accuracy and temporal sampling exist is the Sun. We analyze and model solar variability on timescales relevant for planetary transits (hours to several days) using a variety of components, such as granulation, network (supergranulation), faculae and sunspots. This study extends our successful modeling of solar irradiance variations on days to years timescales to these shorter timescales.

1. Introduction

The most successful method for detecting extrasolar planets to date is based on radial velocity measurements. However, it is essentially limited to giant planets. In order to search for extrasolar terrestrial planets a different technique must be applied. Best suited is the detection of planetary transits. A planetary transit is manifested by a dip in the stellar light curve. The depth of the dip is proportional to the ratio of the surface area of the planet to that of the parent star and is less than 0.01% for Earth-type planets.

However, the majority of stars are variable. Intrinsic variability of the parent star is the dominant source of noise during the planetary transit observations which can lead to spurious detections or mask real ones. An understanding of the origin of stellar variability is therefore important in order to improve the accuracy of such measurements.

In this paper we take the Sun as the closest and best studied star and analyze its variability. Observations of the Sun provide currently the only relevant data set which is long, well sampled and accurate enough for our analysis. We consider solar total and spectral irradiance measurements made by the VIRGO instrument on board the SOHO spacecraft (Fröhlich et al. 1997). Spectral data include measurements in 3 channels: red, green and blue centered at 862nm, 500nm and 402nm respectively. We first analyze variability on time scales of a day and longer and then on shorter time scales. In particular, we distin-

The reconstructed irradiance and the corresponding VIRGO measurements for the period between 1996 and 2002 are shown in Fig. ??. The excellent agreement between the model and data leads to the conclusion that the main driver of the solar irradiance variability at time scales of a day up to, at least, a solar cycle is the magnetic field at the solar surface.

3. Short-term Solar Variability

3.1. Mechanism

The origin of irradiance variations at shorter timescales remains, however, unclear. If they are also related to the Sun's magnetic activity, then they should follow the 11-year cycle. Therefore we have analyzed VIRGO records for the quiet (1996–1997) and active (1999–2000) Sun periods individually. We have applied Fourier and wavelet techniques to the data. Both gave basically the same results, except that the global wavelet power spectrum shows smaller fluctuations due to the smoothing introduced by Morlet wavelets (see Seleznyov et al. 2003 and Solanki et al. 2003 for more details).

The ratio of the wavelet power spectrum for the active Sun period to that for the quiet Sun is shown in Fig. ??. As expected, the ratio is considerably higher than 1 at periods longer than 1–2 days, where magnetic fields dominate the variability. At shorter periods, the ratio is essentially 1 (values below 1 in the 3 colour channels may be an instrumental artifact). This seems to be indicative of a non-magnetic origin of the irradiance variations, with convection being a possible main contributor. At timescales between approximately an hour and a day (which is of particular interest for planetary transits) both mechanisms may play a part.

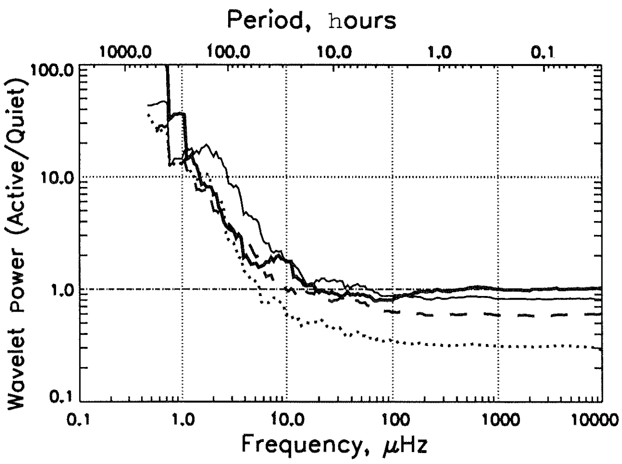

Figure 2. Ratio of wavelet global power spectra of activity maximum to those at activity minimum for the TSI (thick line) and three VIRGO channels: red (thin solid line), green (dashed) and blue (dotted).

that has been derived empirically (Hirzberger et al. 1999). 4) The granular size distribution (Fig. ??b) is also taken in accordance with the observations (Roudier & Muller, 1987). In order to check the importance of these parameters, we have alternately varied each of them. Two other parameters, the total number of granules, N_{tot}, and the brightness contrast between granule and intergranular lanes will only move the irradiance power spectrum up or down, but not influence its slope or shape.

Some results of our modeling are shown in Fig. ??. Lifetime of granules and thickness of the intergranular lanes were varied in Figs. ?? a and b, respectively. Longer lifetimes and/or thinner intergranular lanes lead to a steeper slope of the power below several hours. An increase in granular sizes also moves the turning point of the power towards longer periods.

4. Conclusions

We have analyzed solar irradiance variations on timescales between minutes and a solar cycle. Whereas on timescales of a few days and longer, the main mechanism of variations is solar magnetic activity, on shorter timescales convection becomes more and more important. Our simple model implies that granule lifetime and diameters, relative fractions of splitting and dissolving granules as well as thickness of intergranular lanes are important factors determining the shape of the power spectrum at periods shorter than several hours. The crossover between magnetic and convective signatures coincides with the frequency band of most interest for planetary transit observations. Further improvement of the granulation model and combining it with the model due to magnetic field evolution is therefore needed, followed by a generalization to other stars.

References

Fligge, M., Solanki, S.K., Meuner, N. & Unruh, Y.C., 2000, ESA-SP, 463, 117
Fröhlich, C., Andersen, B.N., Appourchaux, T. et al., 1997, Sol.Phys., 170, 1
Hirzberger, J., Bonet, J.A., Vazquez, M. & Hanslmeier, A., 1999, ApJ 515, 441
Krivova, N.A., Solanki, S.K., Fligge, M. & Unruh, Y.C., 2003, A&A, 399, L1
Krivova, N.A. & Solanki, S.K., 2003, ESA-SP, 535, in press.
Kurucz, R.L., 1992, Rev. Mex. Astron. Astrofis., 23, 187
Roudier, Th. & Muller, R., 1987, Sol.Phys., 107, 11
Seleznyov, A.D., Solanki, S.K. & Krivova, N.A., 2003, ESA-SP, 539, in press.
Solanki, S.K., Seleznyov, A.D., & Krivova, N.A., 2003, ESA-SP, 535, in press
Solanki, S.K., 2002, ESA-SP, 508, 173
Solanki, S.K. & Brigljević, V., 1992, A&A, 262, L29
Unruh, Y.C., Solanki, S.K., & Fligge, M., 1999, A&A, 345, 635

C138

Stars as Suns: Activity, Evolution, and Planets
IAU Symposium, Vol. 219, 2004
A. K. Dupree and A. O. Benz, Eds.

Overview of Slow Mode Oscillations in Hot Coronal Loops Observed by SUMER

T. J. Wang, S. K. Solanki, W. Curdt, and D. E. Innes

Max-Planck Institut für Aeronomie, D-37191 Katlenburg-Lindau, Germany (email:wangtj@linmpi.mpg.de)

Abstract. Doppler shift oscillations in hot active region loops off the limb of the Sun have been detected with the Solar Ultraviolet Measurements of Emitted Radiation (SUMER) spectrometer in the Fe XIX and Fe XXI lines. Various lines of evidence have been found to support that these oscillations are caused by slow magnetoacoustic standing waves in the loops excited by the impulsive injection of hot material to coronal heights. Here we review recent results from observations and MHD simulations on this topic.

1. Introduction

The search for oscillations and waves in coronal loops is strongly motivated by the theories of coronal heating and acceleration of the solar wind. Observations of oscillations in coronal structures may also lead to coronal seismology, from which coronal physical parameters can be obtained.

The imaging observations with SOHO and TRACE in the EUV have definitely detected transverse kink-mode oscillations (e.g. Aschwanden et al. 1999), and propagating slow magneto-acoustic waves (e.g. Berghmans & Clette 1999) in cool (<2 MK) coronal loops. More recently, standing slow-mode oscillations were for the first time discovered by SUMER in hot (> 6 MK) coronal loops (e.g. Wang et al. 2002). In this paper, we review the results on the SUMER loop oscillations.

2. Hot Loop Oscillations

In order to study time variations and dynamics of active region loops, a large number of spectral observations (JOP104) were made by SUMER on SOHO during 1999–2002. The SUMER spectra were recorded with the $300'' \times 4''$ slit at a fixed position off the limb. The generally used spectral window contains several lines formed in the temperature range $10^4 - 10^7$ K, e.g. a relatively cool transition region line Si III $\lambda\,1113$ (0.03–0.06 MK), the coronal line Ca X $\lambda\,557 \times 2$ (0.7 MK) and the flare line Fe XIX $\lambda\,1118$ (6.3 MK). To determine what coronal structures are targeted, other imaging observations from SOHO/EIT, TRACE and Yohkoh/SXT are essential complements.

Figure 1 shows an example in which the slit was located at the top of a hot coronal loop seen in soft X-rays above a limb active region. A single Gaussian

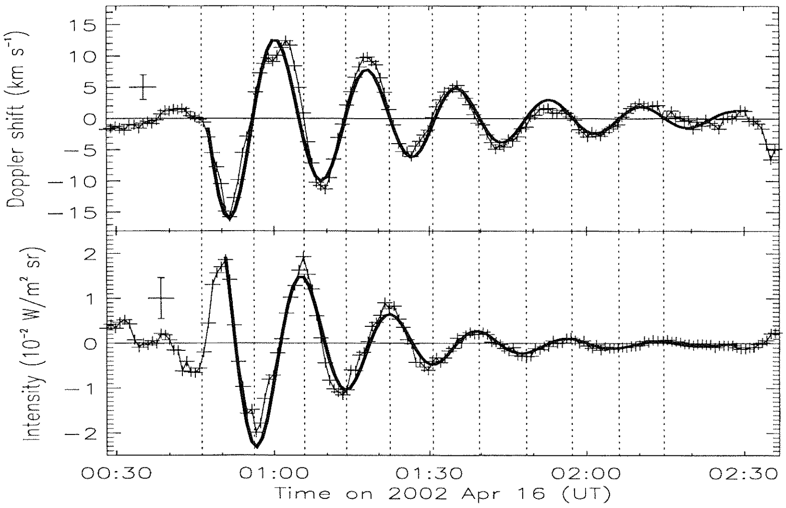

Figure 3. (a) Evolution of Doppler shift and (b) of line-integrated intensity in the Fe XIX line at a distinct region of coherent oscillations along the slit. The thick solid curves are the best fits with a damped sine function. The background shift and the background intensity have been removed, respectively.

the presence of intensity fluctuations with a definite period is not so certain. This could be attributed to the combination of rapid damping of the oscillation and rapid change of the background intensity, which makes it extremely difficult to distill the intensity signal of the oscillations from the observations.

4. Propagating Feature

Observations with a high cadence of 50 s made in April-May 2002 disclosed phase propagation along the slit in some Doppler shift oscillations. The measured propagating speeds cover a range of 8–102 km s^{-1}, with a mean of 43 ± 25 km s^{-1}. Wang et al. (2003b) suggested that these features can be explained by the excitation of the oscillation at a footpoint of an inhomogeneous coronal loop, e.g. a loop with fine structure.

5. Physical Parameters

Figure 4 shows that the histograms of physical parameters for the 54 SUMER oscillations measured by Wang et al. (2003b) are compared with those for the TRACE transverse loop oscillations measured by Aschwanden et al. (2002). The SUMER loop oscillations have periods in the range 7.1–31.1 min with a mean of 17.6±5.4 min, distinctly larger than those for the TRACE case. The decay times in the range 5.7–36.8 min with a mean of 14.6±7.0 min, have a ratio to the period of 0.85±0.35, which is about a factor of 2 shorter than that of TRACE oscillations. The velocity amplitude is comparable. But the derived

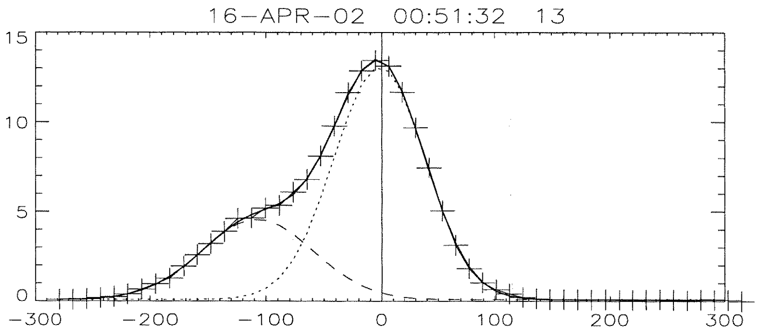

Figure 5. Spectrum of an Fe XIX line at the initial phase of the 16 April 2002 event. The solid curve is the best fit with two Gaussian functions. The dotted line profile corresponds to the main component, and the dashed line profile the initial high Doppler shift component.

thermal conduction due to high temperature of the loop can lead to the rapid damping of slow waves, and the expected scaling of the dissipation time with period agrees well with the observations. A similar simulation by De Moortel & Hood (2003) shows that a large amount of thermal conduction results in the perturbations oscillating with a slower, hybrid period, but not with the "adiabatic" period. Based on a loop model with semi-circular shape and gravity stratification, Mendoza-Briceño, Erdélyi, & Sigalotti (2003) find that stratification results in about 10–20% reduction of the wave-damping time.

References

Aschwanden, M. J., Fletcher, L., Schrijver, C. J., & Alexander, D. 1999, ApJ, 520, 880

Aschwanden, M. J., Pontieu, B. D., Schrijver, C. J., & Title, A. 2002, Sol. Phys, 206, 99

Berghmans, D. & Clette, F. 1999, Sol. Phys, 186, 207

De Moortel, I., & Hood, A. W. 2003, A&A, 408, 755

Mendoza-Briceño, C. A., Erdélyi, R., & Sigalotti, L. D. G. 2003, ApJ, submitted

Ofman, L., & Wang, T. J. 2002, ApJ, 580, L85

Wang, T. J., Solanki, S. K., Curdt, W., Innes, D. E., & Dammasch, I. E. 2002, ApJ, 574, L101

Wang, T. J., Solanki, S. K., Innes, D. E., Curdt, W., & Marsch, E. 2003a, A&A, 402, L17

Wang, T. J., Solanki, S. K., Curdt, W., Innes, D. E., Dammasch, I. E., & Kliem, B. 2003b, A&A, 406, 1105